THE USE OF CONTROL CHARTS TO MONITOR AIR PLANE ACCIDENTS OF THE HELLENIC AIR FORCE

Authors: Vasileios Alevizakos
            – Department of Mathematics, National Technical University of Athens,
              Zografou, Athens, Greece
              basalebiz@yahoo.gr

            Christos Koukouvinos
            – Department of Mathematics, National Technical University of Athens,
              Zografou, Athens, Greece
              ckoukouv@math.ntua.gr

            Petros E. Maravelakis
            – Department of Business Administration, University of Piraeus,
              Piraeus, Greece
              maravel@unipi.gr

Abstract:

• Accidents are unfortunate events that cause economic and/or human losses to individuals, organisations, companies or to the society. Air plane accidents cause both economic and human losses most of the times. In this paper we model the occurrences of air plane accidents using the Poisson distribution. We use control charts, which is the main tool of Statistical Process Control, to identify an out of control situation in the occurrence of air plane accidents. We propose the use of Shewhart and Exponentially Weighted Moving Average control charts and we apply them in real data from the Hellenic Air Force.

1.   INTRODUCTION

Air plane accidents are of major importance since they involve most of the times both human and economic losses. The last decades great effort has been imposed in the safety regulations in all the different aspects of commercial aviation. For example in a series of seven years (2010–2016) there was not any human loss in a crash on a United States-certificated scheduled airline operating anywhere according to official data.

In the case of military air forces things are a bit different. The continuous competitiveness of the air forces leads to the occurrence of air accidents. The accidents of air forces are not in the numbers of the previous decades but still they are a fact. However, in both commercial and military aviation few efforts have been made to monitor the air plane accidents.

Statistical Quality Control (SQC) is a well known collection of methods aiming to continuously improve the quality of a product or a process. Rockwell ([7]) initiated the use of statistical quality control techniques in the field of safety management. Specifically, Rockwell ([7]) dealt with the problem of safety performance measurement. The main tools of SQC methods that are used to monitor critical parameters of a process are the control charts.

The main objective of this paper is to demonstrate how we can use control charts to monitor the air plane accidents. To be more specific, in Section 2 we present the main points of the theory of control charts. We outline the Shewhart and Exponentially Weighted Moving Average (EWMA) Control Charts and the way they are used to monitor a process. In Section 3, we apply the techniques presented in Section 2 in real accident data from the Hellenic Air Force (HAF). Finally, in Section 4 we give some conclusions and guidelines for future research.

2.   CONTROL CHARTS

One of the main objectives of a product or a process is to continuously improve its quality. This goal, in statistical terms, may be expressed as variability reduction. SQC is a popular collection of methods targeting at this purpose and control charts are known to be the main tools to detect shifts in a process. The most popular control charts are the Shewhart charts, the Cumulative Sum (CUSUM) charts and the Exponentially Weighted Moving Average charts (EWMA). Shewhart charts are used to detect large shifts in a process whereas CUSUM and EWMA charts have very good results for small to moderate shifts. Since the CUSUM and EWMA control charts have similar performance, in this paper we confine ourselves to the EWMA chart.

A control chart is a graphical representation of one or more characteristics of the process under investigation. It is the main tool to identify special causes of variability in a process. On the horizontal axis we plot the number of the sample drawn from the process or the time that the sample was inspected. On the vertical axis we plot the value of the characteristic or the characteristics measured for each sample or for the time of the horizontal axis. A straight line connects the successive points indicating the level of the characteristic in time or in successive samples. There are also three usually straight lines that stand for the upper control limit (UCL), the center line (CL) and the lower control limit (LCL).

We deduce that a process operates under control when the line connecting the sequence of points does not cross UCL or LCL. When a point plots outside these limits we conclude that the process is in an out-of-control state and corrective actions must be taken in order to remove the assignable cause that led to this problem.

In the literature, two distinct phases of control charting practice have been discussed (see, e.g. Woodall [12]). In Phase I, charts are used for retrospectively testing whether the process was in-control when the first subgroups were being drawn. In this phase, the charts are used as aids to the practitioner, in bringing a process into a state of statistical control. Once this is accomplished, the control chart is used to define what is meant by statistical control.

In Phase II, control charts are used to test if the process remains in-control when real time subgroups are drawn. In this phase, the control charts are used to monitor the process for a possible shift from the in-control state. The in-control characterization in this phase, is most of the times determined from the values of the process parameters. These values are usually estimated from historical data known to be under control. Usually these data are the ones from Phase I.

The design of a control chart must take into account two contradicting aims. The first one of them refers to the in-control state. In such a case, the control chart should signal (false alarm) as slow as possible. On the other hand, when a process is out-of-control the control chart must signal as soon as possible. The most popular measure to evaluate the performance of a chart concerning the previous two objectives is the average run length (ARL), which is based on the run length (RL) distribution. The number of observations when we plot individual data, or the number of samples when we plot data in subgroups, required for a control chart to signal is a run length (an observation of the RL distribution). The mean of the RL distribution is the ARL, and it can be defined as the average number of observations for a control chart to signal.

Since we deal with a parametric case of control charts we need to assume a distribution for the studied phenomenon. A detailed investigation is given in the following subsection.

2.1. Distribution of air plane accidents

A well known distribution used to model the occurrence of events in time is the Poisson distribution (Kjelln and Albrechtsen [2]). Assume that accidents occur at random points in time, let c be the average number of accidents per unit of time for example one year. Let x be the number of accidents occurring during t time periods. Then, the probability that x accidents will occur during t time periods is equal to

$$P\big(X=x\big) = \frac{(ct)^x}{x!}\,e^{-ct}, \quad x = 0, 1, 2, ...$$

The control charts that will be presented in the following subsections assume that the air plane accidents are well modelled using the Poisson distribution.

2.2. The c chart

Assume that we want to monitor the number of accidents in a fixed time period and let $c > 0$ denote the parameter of the Poisson distribution for simplicity. If the true value of the parameter c is known, the Phase II three sigma control limits will be defined as:

$$\text{UCL} = c + 3\sqrt{c},$$
$$\text{CL} = c,$$
$$\text{LCL} = c - 3\sqrt{c}.$$

If the computed value of LCL is less than zero, then we set $\text{LCL} = 0$.

When the true value of the parameter c is not known, then the average number of accidents in a preliminary sample $(\bar{c})$, is applied as an estimate of c. In this case, the Phase I control limits are defined as follows:

$$\text{UCL} = \bar{c} + 3\sqrt{\bar{c}},$$
$$\text{CL} = \bar{c},$$
$$\text{LCL} = \bar{c} - 3\sqrt{\bar{c}}.$$

The Phase I control limits are considered as trial control limits and the preliminary samples should be examined for lack of control. If there are observations that cross the estimated control limits due to common causes, usually these observations are excluded from the sample and the control limits are recalculated in the usual Phase I analysis (Montgomery [4]).

For the c chart, the probability of type I error (α) is calculated as

$$\alpha = P\Big(X \notin [\text{LCL}, \text{UCL}] \,\big|\, X \sim P(c)\Big)$$
$$= 1 - \big[F_x(\text{UCL}) - F_x(\text{LCL})\big]$$
$$= 1 - \sum_{x=\lceil \text{LCL} \rceil}^{\lfloor \text{UCL} \rfloor} \frac{e^{-c}c^x}{x!}$$

and the in-control ARL (ARL_0) is given by the formula

$$\text{ARL}_0 = \frac{1}{\alpha}.$$

The probability of type II error (β) is

$$\beta = P\Big(\text{LCL} \le X \le \text{UCL} \,\big|\, X \sim P(c^*)\Big)$$
$$= F_x(\text{UCL}) - F_x(\text{LCL})$$
$$= \sum_{x=\lceil \text{LCL} \rceil}^{\lfloor \text{UCL} \rfloor} \frac{e^{-c^*}c^{*x}}{x!},$$

where c^* is the average number of defects displayed in an inspection unit in an out of control process, $\lceil LCL \rceil$ denotes the smaller integer greater than or equal to LCL and $\lfloor UCL \rfloor$ denotes the largest integer less than or equal to UCL. The out-of-control ARL (ARL_1) is given by the formula

$$ARL_1 = \frac{1}{1 - \beta}.$$

We must note here that the same chart presented here can be used to monitor the number of nonconformities or defects in an inspection unit from a repetitive production process.

2.3. The ARL-unbiased c chart

The c chart with $3 - \sigma$ control limits has LCL > 0 if $c > 9$. In case $c \leq 9$, then LCL < 0 and as we mentioned before, we set it equal to zero and a downward shift of the process mean cannot be detected. Denoting as c_0 the in-control mean of the process, Paulino *et al.* [5] proved that for $c_0 > 9$, the ARL of a c chart with $3 - \sigma$ control limits takes its maximum value at the point

$$\delta^*(c_0) = \left[\frac{UCL!}{(LCL - 1)!} \right]^{\frac{1}{UCL - LCL + 1}} - c_0.$$

This means that the maximum of the ARL appears at a point $\delta^*(c_0)$ below the zero, i.e. some ARL_1 values that correspond to downward shifts are larger than the ARL_0. In this case, we say that the chart is ARL-biased.

Many authors, such as Wetherill and Brown [11] and Ryan [8] used quantile-based control limits. In this case LCL and UCL are the largest and smallest non-negative integers, that satisfy

$$P\Big(X < LCL \,\big|\, c = c_0\Big) \leq \alpha_{LCL},$$

$$P\Big(X > UCL \,\big|\, c = c_0\Big) \leq \alpha_{UCL},$$

where $\alpha_{LCL} + \alpha_{UCL} = \alpha$. Using the quantile-based control limits, we have $ARL_0 = 1/\alpha$.

Paulino *et al.* [5] proposed a c chart, named as ARL-unbiased c chart, with quantile-based control limits, that triggers a signal with probability one if the sample number of defects is below LCL or above UCL and probabilities γ_{LCL} and γ_{UCL} if the sample number of defects is equal to LCL and UCL, respectively. The values of probabilities γ_{LCL} and γ_{UCL} can be obtained by solving a system of linear equations. The solution of this system gives

$$(2.1) \qquad\qquad \gamma_{LCL} = \frac{de - bf}{ad - bc},$$

$$(2.2) \qquad\qquad \gamma_{UCL} = \frac{af - ce}{ad - bc},$$

where $a = P\big(X = LCL \,|\, c = c_0\big)$, $b = P\big(X = UCL \,|\, c = c_0\big)$, $c = LCL \cdot P\big(X = LCL \,|\, c = c_0\big)$, $d = UCL \cdot P\big(X = UCL \,|\, c = c_0\big)$, $e = \alpha - 1 + \sum_{x=LCL}^{UCL} P\big(X = x \,|\, c = c_0\big)$ and $f = \alpha \cdot c_0 - c_0 + \sum_{x=LCL}^{UCL} x \cdot P\big(X = x \,|\, c = c_0\big)$. A signal is triggered by the ARL-unbiased c chart with

probability

$$\xi(c^*) = \left[1 - \sum_{x=\text{LCL}}^{\text{UCL}} P\Big(X = x \mid c = c^*\Big)\right]$$
$$+ \gamma_{\text{LCL}} \cdot P\Big(X = \text{LCL} \mid c = c^*\Big) + \gamma_{\text{UCL}} \cdot P\Big(X = \text{UCL} \mid c = c^*\Big)$$

and $\text{ARL}_1 = 1/\xi(c^*)$.

Note that for the c chart, the probability of triggering a signal is equal to $\xi(c^*) = 1 - \sum_{x=\text{LCL}}^{\text{UCL}} P\big(X = x \mid c = c^*\big)$.

2.4. The classical Poisson EWMA control chart (PEWMA)

The EWMA control chart was introduced by Roberts [6]. Borror *et al.* [1] modified this chart to monitor Poisson data. Let $X_1, X_2, \dots$ be i.i.d. Poisson random variables with mean c. When the process is in control, $c = c_0$. The EWMA statistics can be written as follows:

$$(2.3) \qquad\qquad Z_t = \lambda X_t + (1 - \lambda) Z_{t-1}, \qquad t = 1, 2, 3\dots$$

where λ is the smoothing factor, $0 < \lambda \leq 1$ and the starting value is the process target, that is $Z_0 = c_0$. Values of λ in the interval $0.05 \leq \lambda \leq 0.25$ work well in practice, with $\lambda = 0.05$, $\lambda = 0.10$ and $\lambda = 0.20$ being popular choices (Montgomery [4]).

Using the abovementioned definition the mean value of Z_t is

$$E(Z_t) = c_0$$

and the variance of Z_t is

$$\text{Var}(Z_t) = \frac{\lambda}{2 - \lambda}\big[1 - (1 - \lambda)^{2t}\big]c_0.$$

Therefore, the PEWMA control chart is constructed by plotting Z_t versus the sample number i or time t. The center line and control limits for the PEWMA control chart are as follows:

$$(2.4) \qquad\qquad \text{UCL} = c_0 + L\sqrt{\frac{\lambda}{2 - \lambda}\big[1 - (1 - \lambda)^{2t}\big]c_0},$$
$$\text{CL} = c_0,$$
$$(2.5) \qquad\qquad \text{LCL} = c_0 - L\sqrt{\frac{\lambda}{2 - \lambda}\big[1 - (1 - \lambda)^{2t}\big]c_0},$$

where $L > 0$ can be chosen to provide a specified ARL_0. If the computed value of LCL is less than zero, then we set $\text{LCL} = 0$. For large values of t, the control limits converge to the following values:

$$\text{UCL} = c_0 + L\sqrt{\frac{\lambda}{2 - \lambda}c_0},$$
$$\text{CL} = c_0,$$
$$\text{LCL} = c_0 - L\sqrt{\frac{\lambda}{2 - \lambda}c_0}.$$

It is recommended to use the exact control limits of Equations (2.4) and (2.5) for small values of λ (Montgomery [4]).

The PEWMA control chart raises an out-of-control signal when $Z_t < \text{LCL}$ or $Z_t > \text{UCL}$. The ARL values of the PEWMA chart are usually smaller than the ARLs for the c chart and the lower limit for the PEWMA is usually positive so that downward shifts in the process mean can be detected (Borror *et al.* [1]).

2.5. The Poisson Double EWMA (PDEWMA) control chart

Shamma and Shamma [9] developed a double EWMA control chart in an effort to increase the sensitivity of the EWMA control chart to detect small shifts and drifts in a process. Zhang *et al.* [13] extended the idea of the PEWMA chart to create the PDEWMA.

Let $X_1, X_2, \ldots$ be i.i.d. Poisson random variables with mean c. When the process is in control, $c = c_0$. The PDEWMA statistic can be written as follows:

$$Y_t = \lambda X_t + (1 - \lambda)Y_{t-1},$$

(2.6)
$$Z_t = \lambda Y_t + (1 - \lambda)Z_{t-1},$$

where λ is the smoothing factor, $0 < \lambda \leq 1$ and $Y_0 = Z_0 = c_0$. It can be proved that the mean value of Z_t is

$$E(Z_t) = c_0$$

and the variance of Z_t is

$$\text{Var}(Z_t) = \lambda^4 \frac{1 + (1 - \lambda)^2 - (t + 1)^2(1 - \lambda)^{2t} + (2t^2 + 2t - 1)(1 - \lambda)^{2t+2} - t^2(1 - \lambda)^{2t+4}}{\left[1 - (1 - \lambda)^2\right]^3} c_0.$$

The PDEWMA control chart is constructed by plotting Z_t against t. The center line and control limits for the PDEWMA control chart are as follows:

(2.7)
$$\text{UCL} = c_0 + L\sqrt{\text{Var}(Z_t)},$$

$$\text{CL} = c_0,$$

(2.8)
$$\text{LCL} = c_0 - L\sqrt{\text{Var}(Z_t)},$$

where $L > 0$ can be chosen to provide a specified ARL_0 and when the computed value of LCL is less than zero, then we set $\text{LCL} = 0$. For large values of t, the control limits become (see the Appendix A for more details)

$$\text{UCL} = c_0 + L\sqrt{\frac{\lambda(2 - 2\lambda + \lambda^2)}{(2 - \lambda)^3} c_0},$$

$$\text{CL} = c_0,$$

$$\text{LCL} = c_0 - L\sqrt{\frac{\lambda(2 - 2\lambda + \lambda^2)}{(2 - \lambda)^3} c_0}.$$

A process is considered to be out of control if a plotted point lies above the UCL or below the LCL.

Zhang *et al.* [13] concluded that for a PDEWMA chart a smaller value of λ makes the chart more sensitive (with smaller out-of-control ARLs). Furthermore, the PDEWMA chart gives out-of-control signals earlier than the classical PEWMA chart and in particular, the PDEWMA chart is more sensitive to small downward process mean changes than the PEWMA chart, a fact that compensates the complexity of PDEWMA in relation to PEWMA.

2.6. The Poisson EWMA control chart with Head-Start (HS PEWMA)

Lucas and Saccucci [3] introduced the Fast Initial Response (FIR) feature to the EWMA control charts. In this control chart an EWMA control scheme like the one presented in Subsection 2.4 is obtained by simultaneously implementing two one-sided EWMAs, each with a head start (HS). The upper-sided HS PEWMA chart aims at detecting faster increases at the process mean whereas the lower-sided HS PEWMA chart aims at detecting faster decreases at the process mean.

Both the upper and the lower-sided HS PEWMA charts use Equation (2.3) to compute the HS PEWMA statistic. The difference with the PEWMA is the starting value. Specifically, the upper-sided HS PEWMA has a starting value larger than c_0 and lower than UCL (Equation (2.4)) whereas the lower-sided HS PEWMA has a starting value lower than c_0 and larger than LCL (Equation (2.5)).

The rationale of the HS PEWMA control chart is that if the process is initially out-of-control, then the HS PEWMA will give an out of control signal faster than the PEWMA chart. However, if the process is initially in control, HS PEWMA and PEWMA will tend to converge. In this paper, the starting value used in the HS PEWMA chart is the halfway between the mean of the process c_0 and the control limit (UCL and LCL for the upper and lower HS PEWMA control charts, respectively).

2.7. Fast Initial Response Poisson EWMA control chart (FIR PEWMA)

The FIR PEWMA control chart uses an exponentially decreasing adjustment method introduced by Steiner [10] to narrow the distance between the control limits. The control statistic of this chart is the same as in the classical PEWMA (Equation (2.3)) but its time-varying control limits are adjusted as follows:

$$(2.9) \qquad \text{UCL} = c_0 + LF_{\text{adj}}\sqrt{\frac{\lambda}{2-\lambda}\big[1-(1-\lambda)^{2t}\big]c_0},$$

$$\text{CL} = c_0,$$

$$(2.10) \qquad \text{LCL} = c_0 - LF_{\text{adj}}\sqrt{\frac{\lambda}{2-\lambda}\big[1-(1-\lambda)^{2t}\big]c_0},$$

where F_{adj} denotes the FIR adjustment factor and is expressed as

$$F_{\text{adj}} = 1 - (1 - f)^{1 + a(t-1)},$$

$a > 0$ is the adjustment parameter and f is the distance from the starting value with $0 < f \leq 1$. The value of a is chosen, so that the FIR adjustment has a small effect when t gets a suitable (usually not large) value. Steiner [10] suggests to choose a so that the FIR has little effect after about 20 observations. This fact after some calculations leads to $a = \left(-2/\log(1-f) - 1\right)/19$. In this paper, we use $f = 0.5$ and $a = 0.3$.

---

3. APPLICATION OF CONTROL CHARTS AT THE HELLENIC AIR FORCE (HAF) DATA

HAF is tasked with missions that, depending on the situation, conditions and environment, may involve acceptance of a significant and sometimes high risk. Daily challenges in the Aegean sea and many flight hours require continues alertness for these missions to be performed safely. The cost of the accidents, both in the air and on the ground, and the high cost of acquiring new aircraft requires that every effort be made to minimize loss or damage in order to maintain the integrity of the aircraft and the flight ability of HAF. The implementation of this effort is achieved through the detection of risks and the monitoring of accidents.

The main aircraft included in the fleet of HAF is F-16. The annual F-16 accidents for HAF are presented in Table 1.

Table 1: Number of F-16 accidents (1988–2017).

Year	Accidents	Year	Accidents	Year	Accidents
1988	0	1998	0	2008	0
1989	0	1999	0	2009	1
1990	0	2000	1	2010	2
1991	0	2001	1	2011	0
1992	1	2002	0	2012	0
1993	1	2003	1	2013	0
1994	0	2004	2	2014	1
1995	3	2005	0	2015	2
1996	0	2006	1	2016	0
1997	1	2007	1	2017	0

The main objective of this application is to see if there is a shift in the F-16 accidents the last twenty years. For this reason, we use the first ten years to estimate the in-control mean of accidents. Since we have six total accidents the first ten years, we estimate c by

$$\bar{c} = \frac{6}{10} = 0.6.$$

Therefore, the Phase I (trial) control limits are given by

$$\text{UCL} = \bar{c} + 3\sqrt{\bar{c}} = 0.6 + 3\sqrt{0.6} = 2.92,$$

$$\text{CL} = \bar{c} = 0.6,$$

$$\text{LCL} = \bar{c} - 3\sqrt{\bar{c}} = 0.6 - 3\sqrt{0.6} = -1.72 \quad \Rightarrow \quad \text{LCL} = 0.$$

The control chart for the number of accidents of the first ten years is given in Figure 1.
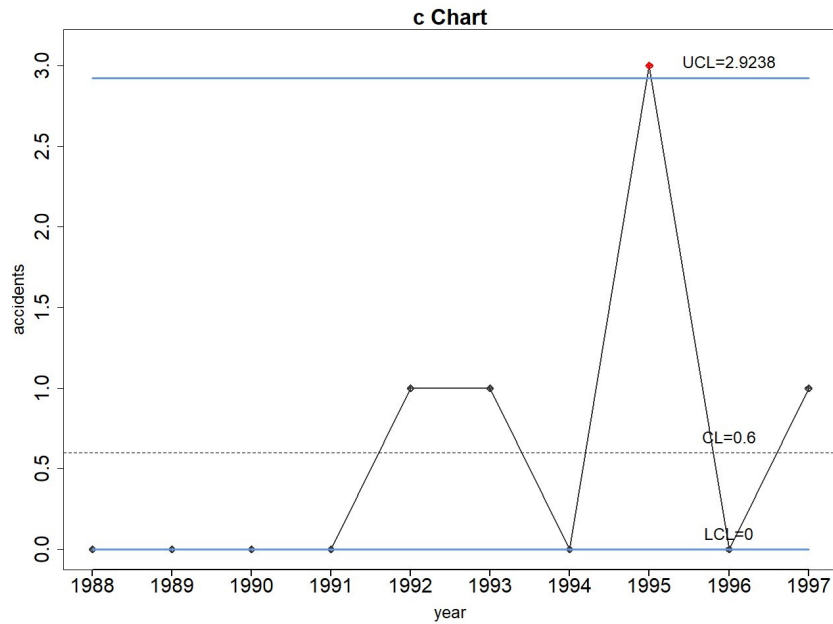
Figure 1: c chart for F-16 accidents (Phase I).

We may see in Figure 1 that there is one point that plots above the UCL (year 1995). We exclude this point and revise the trial control limits. The estimate of c is now computed as

$$\bar{c} = \frac{3}{9} = 0.3333.$$

Using the goodness of fit test ($\chi^2 = 0.7693$ with p value 0.6807), we conclude that the number of accidents from 1988 to 1997 (except of course year 1995) fits the Poisson distribution with parameter $c = 0.3333$. The revised control limits are

$$\text{UCL} = \bar{c} + 3\sqrt{\bar{c}} = 0.3333 + 3\sqrt{0.3333} = 2.0653,$$

$$\text{CL} = \bar{c} = 0.3333,$$

$$\text{LCL} = \bar{c} - 3\sqrt{\bar{c}} = 0.3333 - 3\sqrt{0.3333} = -1.73987 \quad \Rightarrow \quad \text{LCL} = 0.$$

Since all the points are between the control limits we assume that these are the final Phase I control limits that are to be used for the monitoring of the following time periods (years).

For the Phase II charts that follow, we assume that the parameter $\bar{c} = 0.3333$ is the true value of c. However, it is important to note that estimation error often exists in practice, which would result in negative effects on control charts performance.

Let X_t, $t = 1, 2, ..., 20$, be the number of accidents from 1998 to 2017. Using the goodness of fit test ($\chi^2 = 0.8783$ with p value 0.8307), we observe that X_t fits the Poisson distribution with parameter $c^* = 0.65$. These points are plotted on the control chart (Phase II) in Figure 2. The c chart will never be able to detect a downward shift in the mean number of accidents since LCL $= 0$.
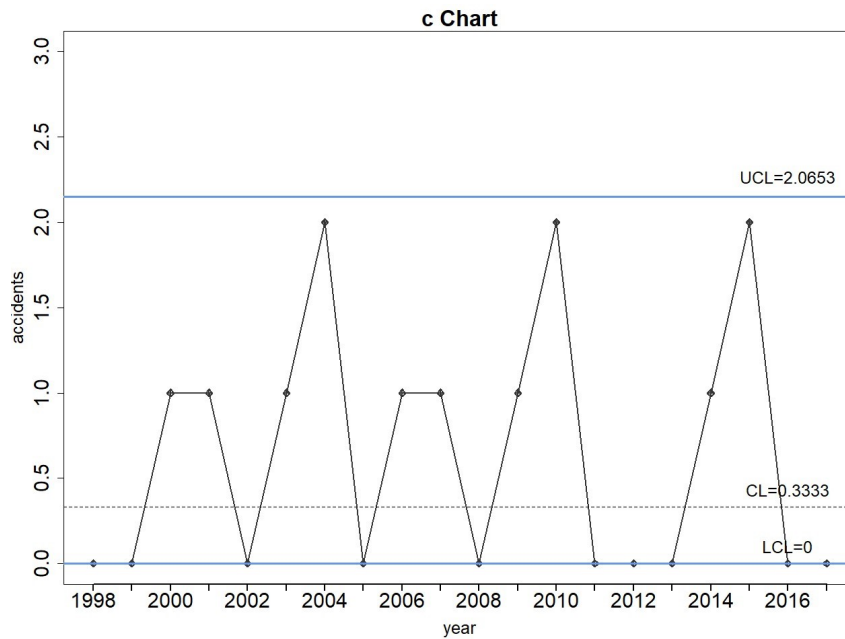
Figure 2: c chart for F-16 accidents (Phase II).

The in-control ARL for this c chart is

$$\text{ARL}_0 = \frac{1}{P\left(X_t > 2 \mid c = 0.3333\right)} = \frac{1}{0.0048163} \cong 207.63.$$

Therefore, if the process is really in-control, we will experience a false out-of-control signal about every 207–208 years. As the process shifts out of control to $c^* = 0.65$, the value of ARL_1 is

$$\text{ARL}_1 = \frac{1}{1 - P\left(0 \leq X_t \leq 2 \mid c^* = 0.65\right)} = \frac{1}{1 - 0.9716577} \cong 35.28$$

and it will take about 35 years to detect this shift with a point crossing the control limits.

In order to calculate the ARL for the PEWMA, PDEWMA, HS PEWMA and FIR PEWMA control charts, we perform Monte Carlo simulations using R. The simulation algorithm is explained as follows:

1. A combination of design parameters (λ, L) is selected and we also set $c_0 = 0.3333$. Then, the control limits of each control chart are calculated using Equations (2.4) and (2.5) for the PEWMA, (2.7) and (2.8) for the PDEWMA and (2.9) and (2.10) for the FIR PEWMA. The control limits for the HS PEWMA are calculated using the methodology described in Subsection 2.6.

2. 25,000 Poisson random numbers are generated with parameters from the previous step.

3. The statistics Z_t, $t = 1, ..., 25,000$ are calculated for each control chart.

4. If $Z_t > \mathrm{LCL}_t$ or $Z_t < \mathrm{UCL}_t$, the process is considered to be in-control, but if $Z_t \leq \mathrm{LCL}_t$ or $Z_t \geq \mathrm{UCL}_t$, a signal is given and the process is considered to be out-of-control. When this event occurs, the simulations stop and the run-length (RL) is recorded.

5. Steps (2)–(4) are repeated 10,000 times. An approximation of the ARL is given by

$$\mathrm{ARL} = \frac{\sum_{t=1}^{N} \mathrm{RL}_t}{N}$$

where N is the number of simulations runs, i.e. in this article $N = 10,000$.

Table 2 shows the performance of various control charts for some combinations of (λ, L). These combinations have been selected so that the ARL_0 of the control charts be close to 207.63. Moreover, the asymptotic control limits are presented in this table. The probabilities γ_{LCL} and γ_{UCL} of the ARL-unbiased c chart are calculated using Equations (2.1) and (2.2), respectively, and they are equal to 0.006171 and $6.523 \cdot 10^{-8}$. "—" is used to indicate that a downward shift cannot be detected, as in some control charts the asymptotic lower control limit is equal to zero. The same results are presented in Appendix B for the case that ARL_0 is close to 370.37. From Table 2, we conclude to the following:

1. PDEWMA control charts, as well as PEWMA, HS PEWMA and FIR PEWMA control charts with $\lambda = 0.05$ can detect a downward shift as they have $\mathrm{LCL} > 0$. Moreover, the ARL-unbiased c chart can detect downward shifts although its LCL is equal to zero. However, these control charts, except from the ARL-unbiased c chart and PDEWMA chart with $\lambda = 0.05$, are ARL-biased, as some ARL_1 values are larger than the ARL_0 values. PDEWMA control chart with $\lambda = 0.05$ is suggested to be used in order to detect a downward shift as its ARL_1 values are smaller than the corresponding values of ARL-unbiased c chart.

2. For $\lambda = 0.05, 0.10$ and 0.15, the PEWMA chart is more efficient than the PDEWMA chart in detecting upward shifts and vice versa for $\lambda = 0.20$. However, Zhang *et al.* [13] showed that PDEWMA chart performs similarly or slightly better than the PEWMA chart in detecting upward shifts considering the in-control mean equal to 4, 8, 12 or 20. We observe different performance of PEWMA and PDEWMA charts for processes where the in-control mean is small.

3. For a specified value of λ, HS PEWMA and FIR PEWMA control charts are more efficient than c chart, ARL-unbiased c chart, PEWMA and PDEWMA control charts in detecting upward shifts. Furthermore, when $\lambda = 0.05$, the HS PEWMA performs similarly with the FIR PEWMA control chart, but when $\lambda = 0.10, 0.15$ or 0.20, the FIR PEWMA is more efficient than the HS PEWMA. For example, when $c^* = 0.65$, the ARL_1 for a HS PEWMA chart with $\lambda = 0.05$ and $L = 2.331$ is 10.83, while the ARL_1 for a FIR PEWMA chart with $\lambda = 0.05$ and $L = 2.315$ is 10.89, the ARL_1 for a PEWMA chart with $\lambda = 0.05$ and $L = 2.261$ is 13.39 and the ARL_1 for a PDEWMA chart with $\lambda = 0.05$ and $L = 1.680$ is 14.95.

Table 2: ARL_1 values for various control charts with $\text{ARL}_0 \cong 207.63$.

shift	c chart $\lambda = 1$ $L = 3$	PEWMA 0.05 2.261	0.10 2.527	0.15 2.780	0.20 2.940	PDEWMA 0.05 1.680	0.10 1.967	0.15 2.140	0.20 2.233
	UCL = 2.065 LCL = 0	0.542 0.124	0.668 0	0.790 0	0.899 0	0.443 0.223	0.518 0.149	0.583 0.084	0.639 0.028
0.15	—	50.64	—	—	—	30.10	39.24	53.83	92.34
0.20	—	90.33	—	—	—	49.85	68.51	99.05	190.76
0.25	—	179.92	—	—	—	94.36	129.61	184.10	336.27
0.30	—	263.86	—	—	—	183.58	211.59	246.79	302.22
0.3333	207.63	207.49	207.56	207.70	207.69	207.44	207.38	207.67	207.48
0.40	126.16	86.94	83.64	89.31	96.31	99.88	102.20	99.29	91.70
0.45	91.92	49.43	49.78	54.28	60.95	55.49	58.30	58.05	54.63
0.50	69.50	31.72	32.96	36.52	41.38	35.69	37.57	37.62	36.20
0.55	54.16	22.23	23.35	26.05	30.02	24.97	26.28	26.36	25.62
0.60	43.26	16.79	17.69	19.65	22.97	18.78	19.60	19.65	19.14
0.65	35.28	13.39	14.14	15.44	17.98	14.95	15.60	15.66	15.26

shift	ARL-unbiased	HS PEWMA $\lambda = 0.05$ $L = 2.331$	0.10 2.549	0.15 2.784	0.20 2.955	FIR PEWMA 0.05 2.315	0.10 2.607	0.15 2.844	0.20 3.013
	UCL = 3 LCL = 0	0.549 0.118	0.671 0	0.791 0	0.902 0	0.547 0.119	0.679 0	0.801 0	0.913 0
0.15	187.61	49.11	—	—	—	52.35	—	—	—
0.20	195.73	91.92	—	—	—	94.68	—	—	—
0.25	202.46	190.56	—	—	—	188.82	—	—	—
0.30	206.73	280.12	—	—	—	272.15	—	—	—
0.3333	207.63	207.40	207.42	207.52	207.45	207.74	207.45	207.63	207.58
0.40	203.55	77.28	80.78	88.65	94.30	78.58	77.05	85.40	89.28
0.45	194.93	42.60	46.97	53.26	58.94	43.42	44.04	49.95	54.30
0.50	182.00	26.54	30.66	35.26	39.50	27.13	28.09	32.27	35.25
0.55	165.94	18.35	21.73	24.94	28.26	18.70	19.45	22.40	24.53
0.60	148.26	13.66	16.37	18.92	21.43	13.88	14.39	16.67	18.21
0.65	130.39	10.83	13.03	14.91	16.68	10.89	11.31	12.88	14.03

The PEWMA control charts for $\lambda = 0.05$ and $\lambda = 0.10$ are shown in Figures 3 and 4, respectively. These two control charts have the same performance since thirteen observations are needed to issue an out of control signal. Theoretically, the average number of observations needed to detect the shift is thirteen and fourteen, respectively (see Table 2).
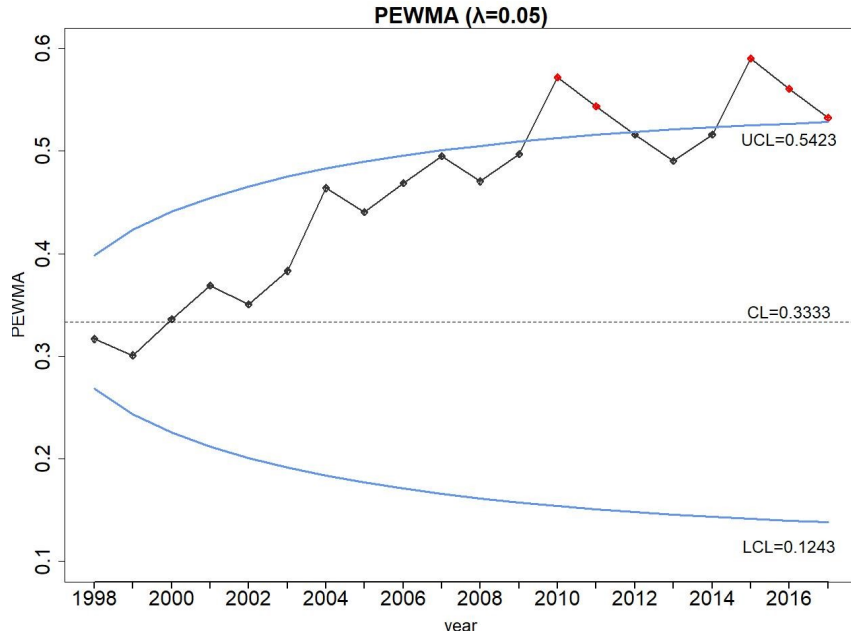
Figure 3: PEWMA ($\lambda = 0.05$).
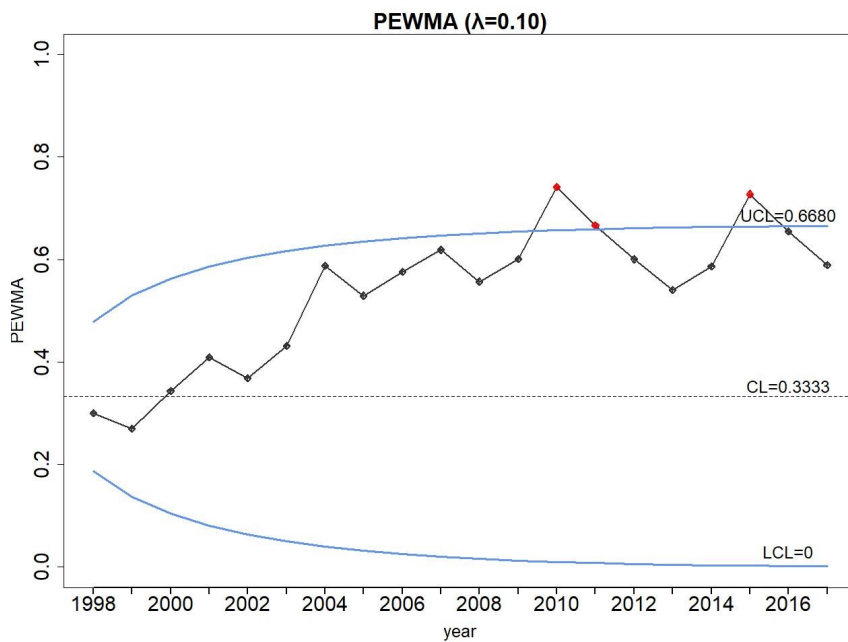
Figure 4: PEWMA ($\lambda = 0.10$).

The PDEWMA control charts for $\lambda = 0.05$ and $\lambda = 0.10$ are shown in Figures 5 and 6, respectively. These control charts have the same performance with the corresponding PEWMA charts as they also need thirteen observations to detect the shift. This value is close to the theoretically ARL_1 given in Table 2.
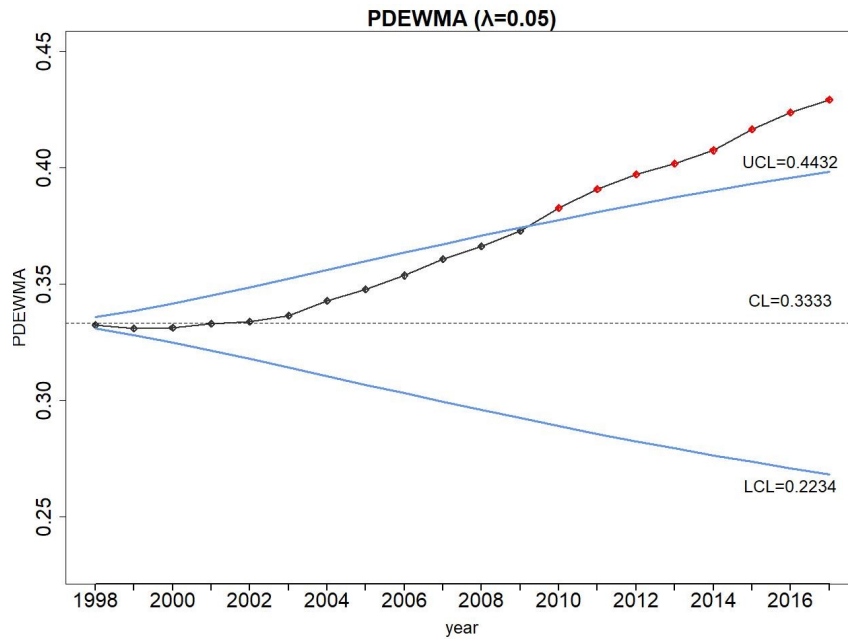
Figure 5: PDEWMA ($\lambda = 0.05$).
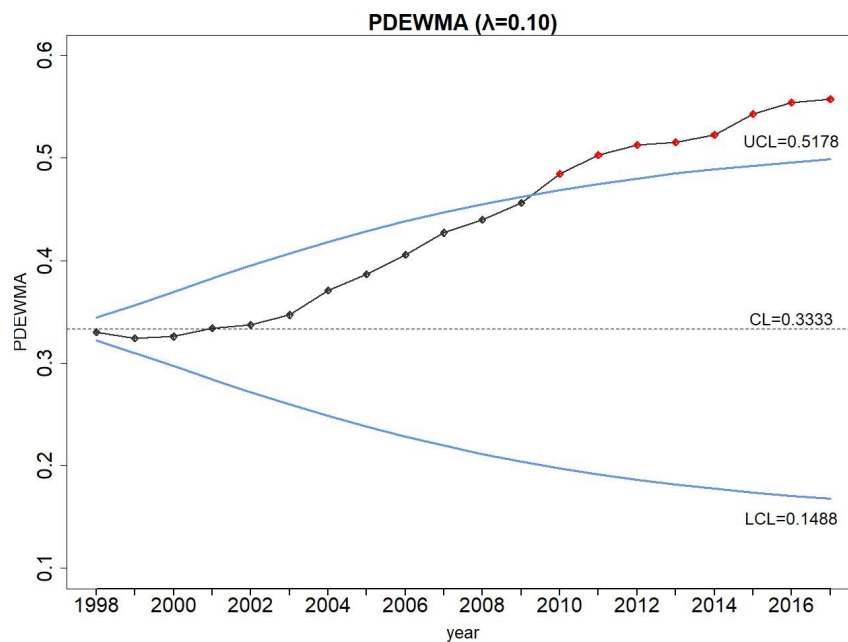
Figure 6: PDEWMA ($\lambda = 0.10$).

In Figure 7, we present the HS PEWMA control chart for $\lambda = 0.05$ when the starting value is halfway between the mean of the process c_0 and the control limit. We notice that the HS PEWMA control chart with $\lambda = 0.05$ detects the shift after ten observations and apparently its performance is much better than all the control charts already presented. Moreover, the theoretical ARL_1 value for this chart is 10.83 which is smaller than all the other competing charts. The HS PEWMA control chart with $\lambda = 0.10$ (Figure 8) detects the shift after thirteen observations, having similar performance to the corresponding PEWMA charts. Note also that as the value of λ increases, the two plotted statistics converge faster.
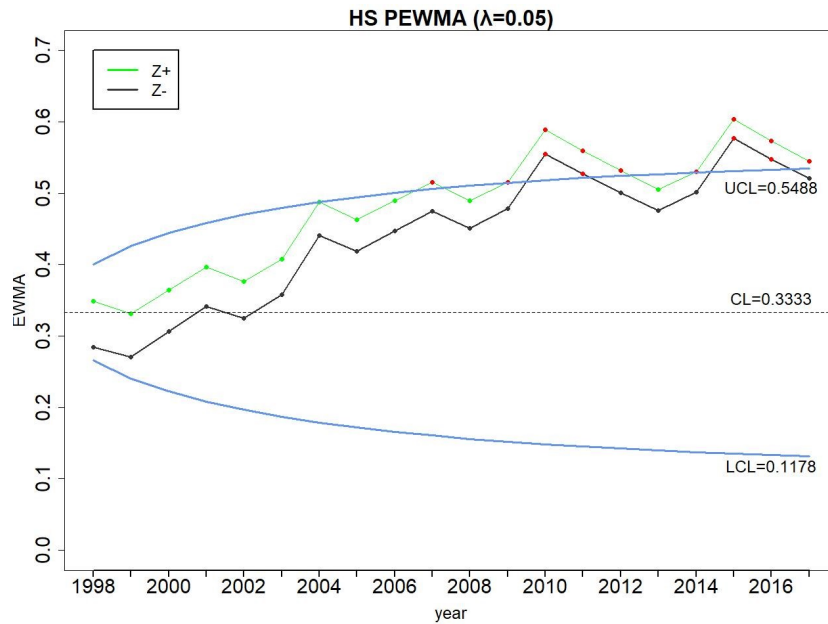
Figure 7: HS PEWMA ($\lambda = 0.05$).
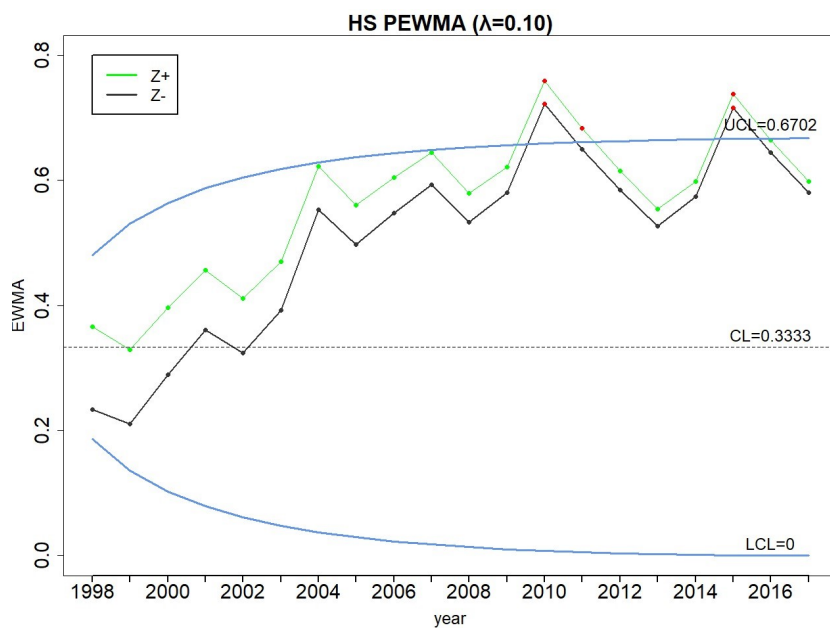
Figure 8: HS PEWMA ($\lambda = 0.10$).

In Figures 9 and 10 we present the FIR PEWMA for $\lambda = 0.05$ and $\lambda = 0.10$, respectively. We deduce that the FIR PEWMA chart with $\lambda = 0.05$ detects the shift after ten observations and therefore its performance is the same as HS PEWMA chart. On the other hand, FIR PEWMA control chart with $\lambda = 0.10$ detects the shift after thirteen observations and its performance is the same as the other three corresponding charts. In both Figures 9 and 10, the ARL_1 value is close to theoretical values given in Table 2.
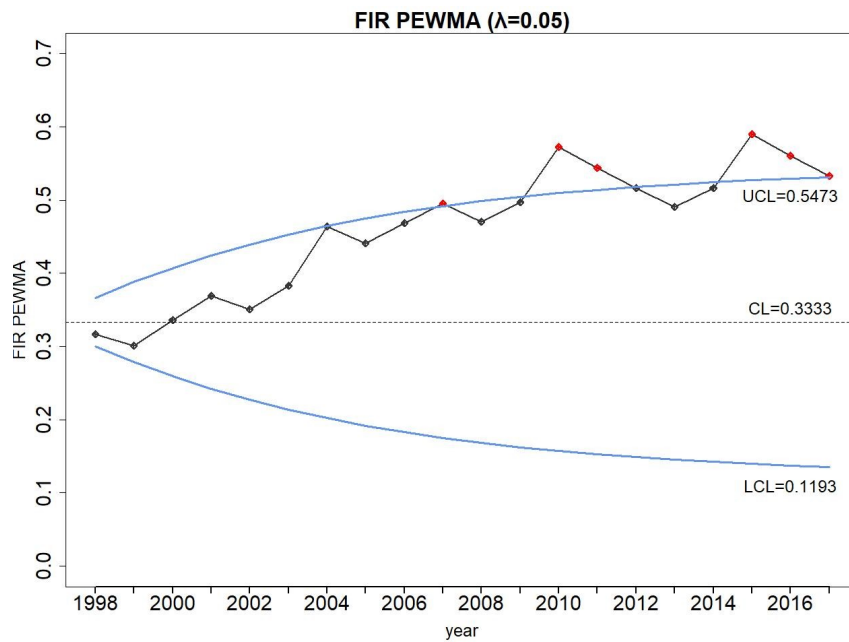
Figure 9: FIR PEWMA ($\lambda = 0.05$).
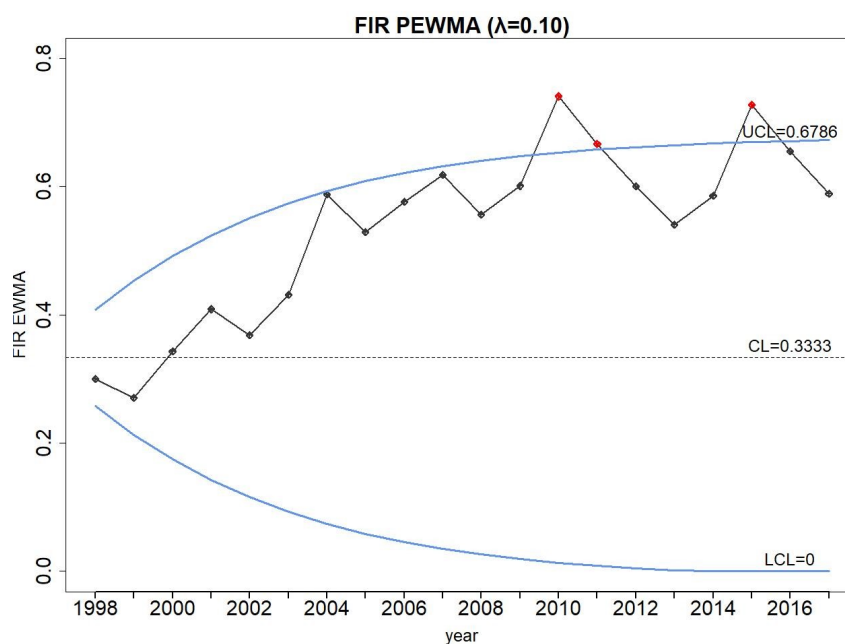
Figure 10: FIR PEWMA ($\lambda = 0.10$).

To sum up, the results show that PEWMA charts with HS or FIR feature and $\lambda = 0.05$ detect the shift more quickly than the other charts. Since, according to the HS PEWMA and FIR PEWMA with $\lambda = 0.05$ control charts, there is a shift in observation ten, management should search for an assignable cause at year 2007.

4.　CONCLUSIONS

In this paper we model air plane accidents using the Poisson distribution and we monitor these accidents using Shewhart and EWMA control charts. We present several different control charts and we discuss their implementation both theoretically and practically. We apply these charts to the HAF Data and we draw useful conclusions.

Process monitoring with control charts is an important component within an overall process evaluation and improvement in air force industry. Future research will focus on more sophisticated control charts that can be applied in similar data taking into account the fact that less accidents occur as the air force industry incorporates new technologies.

A.　APPENDIX

We have

$$\mathrm{Var}(Z_t) = \lambda^4 \frac{1 + (1-\lambda)^2 - (t+1)^2(1-\lambda)^{2t} + (2t^2 + 2t - 1)(1-\lambda)^{2t+2} - t^2(1-\lambda)^{2t+4}}{\left[1 - (1-\lambda)^2\right]^3} c_0$$

and we will prove that $\displaystyle\lim_{t\to\infty} \mathrm{Var}(Z_t) = \frac{\lambda(2 - 2\lambda + \lambda^2)}{(2-\lambda)^3} c_0$.

First of all, for $\lambda = 1$, the PDEWMA, as well as the PEWMA, reduces to a c chart and $\mathrm{Var}(Z_t) = c_0$.

For $\lambda < 1$ and applying L'Hospital's rule, we have

$$\lim_{t\to\infty} (t+1)^2(1-\lambda)^{2t} = \lim_{t\to\infty} \frac{(t+1)^2}{\left(\frac{1}{1-\lambda}\right)^{2t}} = \lim_{t\to\infty} \frac{2t+2}{2\left(\frac{1}{1-\lambda}\right)^{2t} \ln\left(\frac{1}{1-\lambda}\right)}$$

$$= \lim_{t\to\infty} \frac{1}{2\left(\frac{1}{1-\lambda}\right)^{2t} \left(\ln\left(\frac{1}{1-\lambda}\right)\right)^2} = 0.$$

In the same way, we have $\displaystyle\lim_{t\to\infty} (2t^2 + 2t - 1)(1-\lambda)^{2t} = \lim_{t\to\infty} t^2(1-\lambda)^{2t+4} = 0$.

So, $\displaystyle\lim_{t\to\infty} \mathrm{Var}(Z_t) = \lambda^4 \frac{1 + (1-\lambda)^2}{\left[1 - (1-\lambda)^2\right]^3} c_0 = \lambda^4 \frac{2 - 2\lambda + \lambda^2}{\left[\lambda(2-\lambda)\right]^3} c_0 = \lambda \frac{2 - 2\lambda + \lambda^2}{(2-\lambda)^3} c_0.$

B.   APPENDIX

Table 3: ARL_1 values for various control charts with $ARL_0 \cong 370.37$.

	c chart	PEWMA				PDEWMA			
shift	$\lambda = 1$ $L = 3$	0.05 2.520	0.10 2.886	0.15 3.112	0.20 3.288	0.05 1.931	0.10 2.224	0.15 2.397	0.20 2.530
	UCL = 2.065 LCL = 0	0.566 0.100	0.716 0	0.845 0	0.966 0	0.460 0.207	0.542 0.125	0.613 0.054	0.680 0
0.15	—	75.31	—	—	—	39.57	55.48	93.30	—
0.20	—	158.08	—	—	—	68.18	105.69	207.60	—
0.25	—	392.14	—	—	—	141.56	233.07	457.80	—
0.30	—	585.13	—	—	—	322.63	423.92	552.79	—
0.3333	207.63	370.19	368.34	370.13	370.51	370.63	370.29	370.81	370.30
0.40	126.16	118.72	127.89	143.78	155.09	141.42	143.20	137.25	135.75
0.45	91.92	63.54	72.45	84.66	94.21	72.47	75.79	76.56	76.38
0.50	69.50	39.62	45.90	55.06	62.10	44.59	46.96	47.70	48.98
0.55	54.16	27.21	31.42	38.29	43.41	30.49	31.81	32.38	33.54
0.60	43.26	19.99	22.87	28.16	31.87	22.31	23.13	23.49	24.21
0.65	35.28	15.72	17.61	21.58	24.48	17.52	18.07	18.19	18.71

	ARL-unbiased	HS PEWMA				FIR PEWMA			
shift		$\lambda = 0.05$ $L = 2.551$	0.10 2.895	0.15 3.131	0.20 3.303	0.05 2.582	0.10 2.935	0.15 3.170	0.20 3.336
	UCL = 4 LCL = 0	0.569 0.097	0.717 0	0.848 0	0.969 0	0.572 0.095	0.722 0	0.854 0	0.975 0
0.15	334.31	74.50	—	—	—	80.75	—	—	—
0.20	348.86	163.55	—	—	—	175.61	—	—	—
0.25	360.99	421.06	—	—	—	452.65	—	—	—
0.30	368.72	614.36	—	—	—	639.74	—	—	—
0.3333	370.37	370.87	370.71	370.65	370.80	370.43	370.60	370.37	370.12
0.40	362.87	113.36	127.20	139.00	151.09	109.94	121.22	135.30	145.38
0.45	346.93	58.86	70.27	80.53	90.26	56.24	65.95	76.19	84.75
0.50	322.95	35.78	43.58	50.99	58.22	33.96	40.61	47.42	53.40
0.55	293.14	24.27	29.73	34.93	39.97	22.72	27.12	31.68	35.96
0.60	260.38	17.80	21.65	25.23	28.91	16.37	19.43	22.68	25.53
0.65	227.39	13.86	16.69	19.18	21.91	12.70	14.75	17.05	19.11

ACKNOWLEDGMENTS

REFERENCES

[1]   BORROR, C.M.; CHAMP, C.W. and RIGDON, S.E. (1998). Poisson EWMA control charts, *Journal of Quality Technology*, **30**, 352–361.

[2]   KJELLN, U. and ALBRECHTSEN, E. (2017). *Prevention of Accidents and Unwanted Occurrences, Theory, Methods, and Tools in Safety Management*, CRC Press.

[3]   LUCAS, J.M. and SACCUCCI, M.S. (1990). Exponentially weighted moving average control schemes: properties and enhancements, *Technometrics*, **32**, 1–12.

[4]   MONTGOMERY, D.C. (2013). *Introduction to Statistical Quality Control*, Wiley.

[5]   PAULINO, S.; MORAIS, M.C. and KNOTH, S. (2016). An ARL-unbiased c-chart, *Quality and Reliability Engineering International*, **32**, 2847–2858.

[6]   ROBERTS, S.W. (1959). Control chart tests based on geometric moving averages, *Technometrics*, **1**, 239–250.

[7]   ROCKWELL, T.H. (1959). Safety performance measurement, *Journal of Industrial Engineering*, **10**, 12–16.

[8]   RYAN, T.P. (2011). *Statistical Methods for Quality Improvement*, 3rd Edn., Wiley.

[9]   SHAMMA, S.E. and SHAMMA, A.K. (1992). Development and evaluation of control charts using double exponentially weighted moving averages, *International Journal of Quality & Reliability*, **9**, 18–25.

[10]   STEINER, S.H. (1999). EWMA control charts with time-varying control limits and fast initial response, *Journal of Quality Technology*, **31**, 75–86.

[11]   WETHERILL, G.B. and BROWN, D.W. (1991). *Statistical Process Control: Theory and Practice*, Chapman and Hall.

[12]   WOODALL, W.H. (2000). Controversies and contradictions in statistical process control, *Journal of Quality Technology*, **32**, 341–350.

[13]   ZHANG, L.; GOVINDARAJU, K.; LAI, C.D. and BEBBINGTON, M.S. (2003). Poisson DEWMA control chart, *Communication in Statistics – Simulation and Computation*, **32**, 1265–1283.